New insight into the key proteins and pathways involved in the metastasis of colorectal carcinoma

GUAN-ZHEN YU[1], YING CHEN[2], YA-QIU LONG[3], DONG DONG[4], XIAO-LAN MU[5] and JIE-JUN WANG[1]

Departments of [1]Oncology and [2]Pathology, Changzheng Hospital; [3]Shanghai Institute for Biological Sciences, Chinese Academy of Sciences; [4]National Engineering Center for Biochip at Shanghai; [5]Genminix Informatics Ltd. Co, Shanghai, P.R. China

Received November 28, 2007; Accepted January 12, 2008

Abstract. Metastasis-associated genomic alterations have been recognized to play a critical role in tumor metastasis. Primary and metastatic tumor cells in mice and tumors in a patient were studied by cDNA array analysis. Selected genes were determined by RT-PCR and immunohistochemistry. Pathways on changed genes were statistically analyzed. The function of Grb2 was determined by *in vitro* wound assay. Nodal metastatic cells had a stronger ability of growth and metastasis than primary tumor cells. A total of 376 genes showed a different expression between primary and metastatic cells. The expression of Grb2 and genes in the Grb2-mediated pathways was significantly elevated in the metastases. Elevated levels of Grb2 expression in metastases were related to the distant metastasis of colorectal carcinoma. Blocking the Grb2-SH2 domain signaling transduction inhibited cell motility. Metastasis-associated genes identified by cDNA and tissue microarrays provide potentially valuable information on the metastasis of colorectal tumors. Overexpression of Grb2 may contribute to tumor growth, invasiveness and metastasis.

Introduction

Colorectal carcinoma is one of the most common cancers in the world. Despite advances in diagnosis and treatment, it remains a severe threat to life due to metastasis and associated complications. Significant improvements have been made on the primary tumor thanks to the ongoing new chemotherapeutic agents and improved drug effectiveness; however, almost all patients suffer from fatal metastasis in the end. Therefore, it is essential to gain a comprehensive understanding of the mechanisms of colorectal cancer progression towards metastasis.

At the molecular level, the activation of oncogenes and the inactivation of tumor suppressor genes contribute to the development of colorectal carcinoma. However, in the progression towards metastasis, two distinct classes of genes, metastasis activator (or metastasis promoting) genes and metastasis suppressor genes, may be much more important (1). Nevertheless, how these genetic alterations result in the metastasis of colorectal carcinomas remains unclear. It is well established that the accumulation of mutant genes during the development of metastatic cells tends to be accompanied by other genetic and epigenetic changes including the loss of heterozygosity (2), aberrant promoter methylation and/or gene amplifications, all of which can alter gene expression profiles. Therefore, genome-wide monitoring of gene expression is of great importance in order to disclose the numerous diverse events associated with metastasis.

Previous studies were usually based on the comparison of two kinds of cells of different metastatic potentials and/or between the primary tumor cells and the secondary metastatic cells from the same/different patients. However, cells from primary tumor cells may show a different gene expression profile after long-term passages (3). Thus, cell lines cannot represent the original cancer cells in the patients. Tumor tissues include too many non-malignant cells, such as normal epithelial cells and stroma cells, which affect tumor cell growth and migration (4). To detect exact differences between primary tumor cells and metastatic cells, we implanted primary tumor cells and metastatic tumor cells into the subcutis of nude mice, where tumor cells grow faster than in other sites and pure tumor cells can be obtained. We performed laser microdissection (LMD) to collect malignant cells. Then, we compared gene profiles between primary tumor cells and metastatic tumor cells by cDNA microarray and screened gene products by immunohistochemistry (IHC) and tissue microarray (TMA). The P-value of the two-side Fisher's exact test for the Gene Ontology (GO) category was used to identify significant GO categories and genes and finally possible pathways related to metastasis were explored by using oncogene pathway-analysis.

Correspondence to: Dr Jie-jun Wang, Department of Oncology, Changzheng Hospital, Shanghai, P.R. China
E-mail: qiaoshanqian@yahoo.com.cn

Key words: colorectal carcinoma, metastasis, pathway

Materials and methods

Tissue samples and cell line. One patient with advanced gastric carcinoma was taken into account. Fresh tissues at 5 points of the primary tumor (one at the center, four surrounding the tumor) and 5 metastatic lymph nodes were separately digested into single cells and then individually implanted into the subcutis of 10 BALB/c nude mice (Chinese Academy of Science) within 30 min after those tissues were excised from this patient. Two weeks later, tumor tissues were enucleated from the mice. For the LMD, frozen section slides from the same patient were fixed in 70% ethanol for 30 sec, stained with H&E and after dehydration, the sections were dissected with the LMD system (Source of the system). Cells (10,000-20,000) were collected for the total RNA extraction. Then, the above two cell types were analyzed by cDNA array. Another 34 gastric tumors and corresponding tissues (normal mucosa and nodal metastases) were formalin-fixed and paraffin-embedded (from Shanghai Hospital) and used to construct tissue microarray. Tumors were characterized according to the TNM system, differentiation, types, and histopathological gradation according to the WHO standards. A human colorectal cancer cell line SW620 (ATCC CCL-227, USA) was used for a subsequent study, such as investigating the function of genes from cDNA array.

cDNA expression array. Commercially available cDNA expression arrays (Human 14K cDNA Chip V2.0, Shanghai Biochip Co., Ltd. China) were used to compare the gene expression levels between the two types of cancer tissue cells (primary and metastatic cancer cells). This cDNA microarray contains 13824 genes, 10 positive controls and six negative controls.

RNA extraction, cDNA synthesis and hybridization. Total RNAs were extracted from each sample of primary tumor and metastatic tumor tissues collected from the implanted nude mice into 350 μl of RLT lysis buffer (Qiagen, Hilden, Germany). The RNAs were purified with an RNeasy® mini kit (Qiagen). A 50 μg aliquot of RNA was reversed into cDNA and labeled with Cy3-dCTP or Cy5-dCTP. The hybridization was performed as described previously (7,8). Signal intensities of Cy3 and Cy5 from the 13824 spots were qualified and analyzed by substituting backgrounds, using Array Vision software (Imaging Research, Inc, St. Catharines, Ontario, Canada). Subsequently, each signal was normalized so that the average ratio (Cy3:Cy5) of the 10 housekeeping gene signals would be 1.0 and the value of the root ($Cy3^2$+$Cy5^2$) of each signal would be kept through the normalization. Each spot was individually visualized and those false-positive results due to the excessive background or other hybridization artifacts were eliminated from the analysis. For ratio calculation, we obtained the average of signal intensities of Cy3:Cy5 of each spot and the ratio >2 or <0.5 was defined as the cut-off benchmark to determine the up-regulated or down-regulated genes. Only genes that were shown in both animal models and LMD were selected for further study.

Gene ontology analysis. GoMiner arithmetic was applied to GO analysis. Two-side Fisher's exact test was used for the analysis of the GO category and the false discovery rate (FDR) was used to correct the P-value. We chose only GO categories that had a P-value of <0.05 (Log_{10} (p)<-1.3) and an FDR of <0.05. Within the significant category, the enrichment Re was given by Re = $(n_f/n)/(N_f/N)$, where n_f was the number of flagged genes within the particular category (i.e. genes whose expression levels are considered to be changed beyond a given threshold), n was the total number of genes within that same category, N_f was the number of flagged genes in the entire microarray and N was the total number of genes in the microarray.

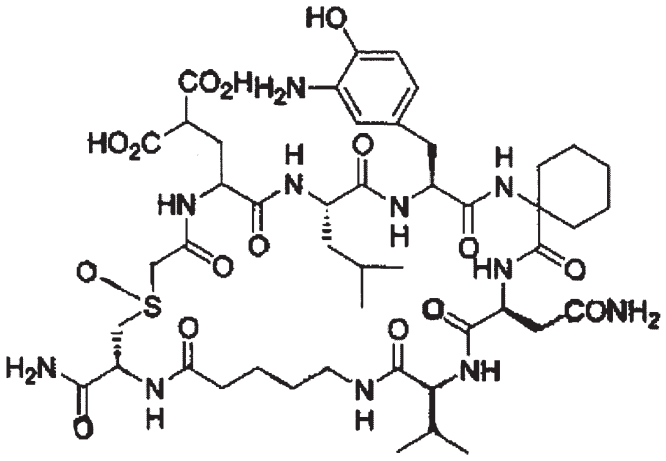

Figure 1. Chemical structure of a Grb2-SH2 domain-binding antagonist.

Real-time RT-PCR. cDNA from 5 μg of total RNA was synthesized using AMV (Avian myeloblastosis virus) reverse transcriptase (Takara, Japan). Each single-stranded cDNA was diluted for subsequent PCR amplification by monitoring GAPDH as a quantitative control. Real-time RT-PCR was carried out using by SYBR Premix Ex Taq (Perfect real-time) kit (Takara) in the Rotor Gene 3000 system (Corbet Research, Sydney, Australia). Results were analyzed by Rotor Gene 5.0 software.

Tissue microarray. The metastasis-related TMA was constructed as described previously (5). The TMAs consisted of 1 normal mucosa, 2 primary tumors and 2 or 3 nodal metastatic tumors from each invasive gastrointestinal cancer case. All the cores from one patient were placed in a line.

Immunohistochemistry. The expression of S100A4, Grb2, EPHB2, KRT20 and KISS1 (according to the higher ratio and enrichment of S100A4 and Grb2, the lower ratio and enrichment of EPHB2, KRT20 and KISS1) in normal adjacent-cancer tissues, primary tumors and metastases was analyzed by using TMA and IHC. Preparations were examined with an En Vision kit (Dako, Denmark) according to a standard protocol. The products of the above genes were detected using commercial antibodies against S100A4 (Dako, Lot118, Denmark), Grb2 (Genex Bioscience, GEA7033-1, USA), EPHB2 (Genex Bioscience, GEA8007, USA), KRT20 (Antibody Diagnostica Inc, K-0343, USA), and KISS1 (Santa Cruz, sc-15400, USA). Two observers (Y.G.Z. and C.Y.)

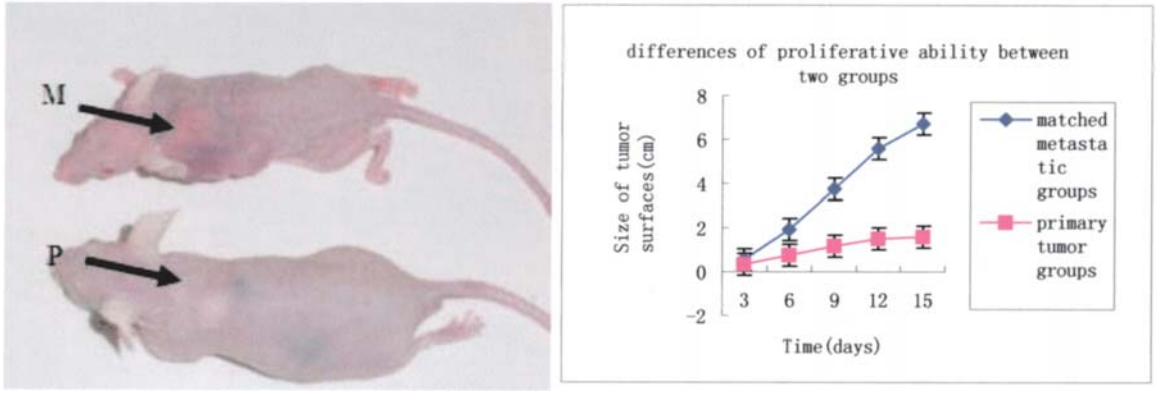

Figure 2. Differences in proliferation between primary tumor and matched metastatic groups. M, one of the metastatic groups; P, one of the primary tumor groups.

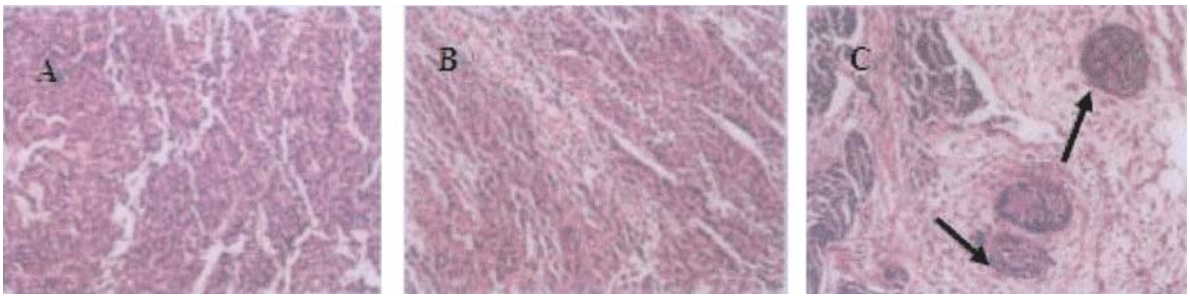

Figure 3. Pure cells from primary tumors and metastatic tissues after being implanted in nude mice. A, primary tumor cells; B, metastatic cells; C, vascular invasion (arrows).

evaluated the staining results. A mean percentage of positive tumor cells was determined in at least five areas at x400 magnification and assigned a grade from 0 to 100. The intensity of the immunostaining was scored as follows: weak, 1^+; moderate, 2^+; and intense, 3^+. The percentage of positive tumor cells and the staining intensity were multiplied to produce a weighted score for each case. The theoretical limits of the scores ranged from 0 (0% of cells staining) to 300 (100% of the cells staining at 3^+ intensity). For the convenience of comparing the differences in the expression levels between tissues and statistical analysis, a dichotomy (negative and positive) was made for each antibody. The cut-off points were raised on the scores, i.e. negative, ≤75% and positive, >75%.

Grb2-SH2 domain-binding antagonists and in vitro wound assay. The synthesis of a Grb2-SH2 domain-binding antagonist (not commercially) was performed as reported previously (6). Sulfoxide-cyclized peptidomimetic displays potent binding with the Grb2-SH2 domain with an IC_{50} value of 58 nM (Fig. 1).

The SW620 cells at the center of the plate were scratched away, washed and incubated in a serum-free culture medium for 12 h. The cells were then treated with the Grb2-SH2 domain-binding antagonist in the cell motility assay. The Grb2-SH2 antagonist was added to the cells at the final concentrations of 0, 10, 30, 50 and 100 mM, respectively.

Statistical analysis. The SPSS 11.0 software package for Windows (SPSS Inc., Chicago, IL) was used for all statistical analysis. IHC data were analyzed by the χ^2 test. A P-value of <0.05 was considered statistically significant.

Results

Macroscopic and histopathological findings. Tumors in nude mice implanted with metastatic cells grew more rapidly than those implanted with primary tumor cells (Fig. 2). The whole tumor tissues were enriched with cancer cells and some inflammatory cells, without obvious stroma cells and epithelial cells of blood/lymph vessels in the primary tumor or in the center of the metastatic tumor. Furthermore, cancer cells in the implanted metastatic tumor penetrated through the basement membrane into the surrounding areas (such as muscles) and vessels (Fig. 3) and formed distant tumor nodules. However, tumors in nude mice implanted primary tumor grew locally and had a complete basement membrane.

cDNA microarray and gene ontology analysis findings. Genes with changed expression in every spot were defined as the commonly up-regulated or down-regulated genes. According to the ratio value, 540 genes were up-regulated and 787 genes were down-regulated. We then examined the significant GO categories and genes by GO analysis. A P-value of <0.05 ($\log_{10\ (p)}$ <-1.3) and an FDR of <0.05 in the two-side Fisher's exact test were selected as the significant criteria. Finally,

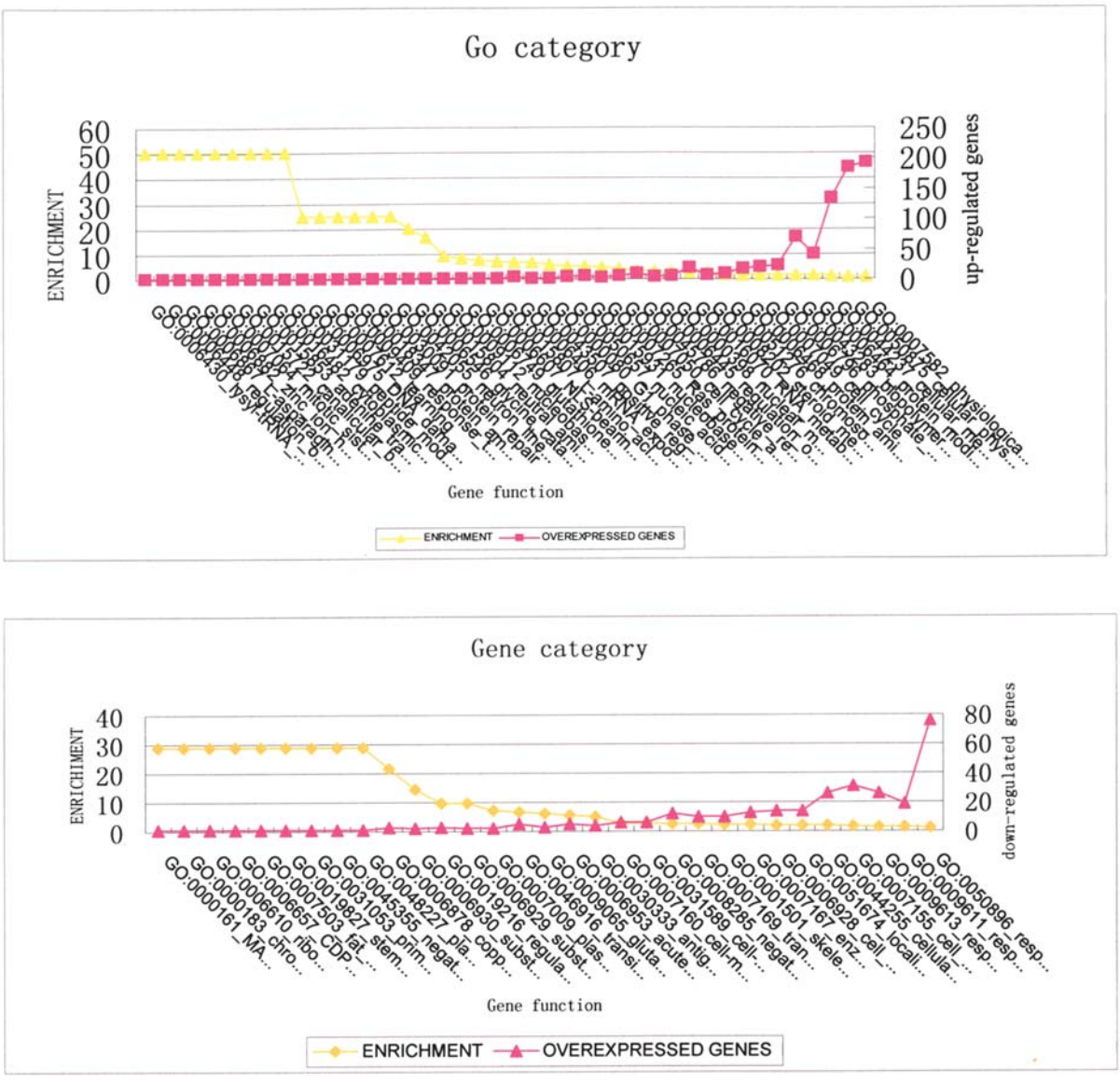

Figure 4. Genes (376) from two groups were sorted into functional categories based on data provided by the GenBank or in the literature.

190 genes fell into the group of the up-regulated genes, while 186 genes fell into the group of the down-regulated genes. These genes were sorted by the enrichment of GO categories (Fig. 4, Table I).

Concordance of cDNA microarray with real-time RT-PCR and TMA. To examine the reliability of our microarray data, we selected six up-regulated genes (GrB2, S100A4, LCK, BMP7, ITPR2 and MFNG) and four down-regulated genes (KRT20, MUCIN3B, KISS1 and EPHB2) and investigated their expression levels by real-time RT-PCR using the same RNA samples that had been used for microarray analysis. The results of real-time RT-PCR were consistent with those from the cDNA microarray data in 8 of the 10 genes (Fig. 5). Another two had a coincident tendency with the microarray data. Furthermore, to investigate the concordance between the protein levels and results obtained by cDNA microarray as well as RT-PCR, TMA was constructed, which contained 35 tumors and corresponding normal and metastatic tissues (Fig. 6A and B). Subsequently, we selected five proteins (GrB2, S100A4, KRT20, KISS1 and EPHB2) to detect their expression levels using TMA and IHC. It was revealed that the levels of GrB2 and S100A4 were higher in metastases than in primary tumors (22/35, 62.9% and 14/35, 40%, respectively), while the levels of KRT20, KISS1 and EPHB2 were significantly lower, or even undetectable, in metastases than in primary tumors (19/35, 54.3%, 24/35, 68.6% and 17/35, 48.6%, respectively) (Table II, Fig. 7).

Grb2-mediated pathways are related to metastasis. In our experiment, we found that the ratio of Grb2 in the metastatic cells was 70 times higher than that in the primary tumor cells and its enrichment was also higher in all the data. The elevated levels of Grb2 were seen in the metastases and were related to liver metastases ($P<0.05$) (Table III). Thus, we used Grb2 as a target to study possible pathways that contribute to metastasis. Proteins in the Grb2-mediated *Ras*, *Akt* and *RHo* pathways changed more markedly and frequently between the metastasis group and the primary tumor group. Most of the genes involved in these pathways were evaluated or declined (Fig. 8).

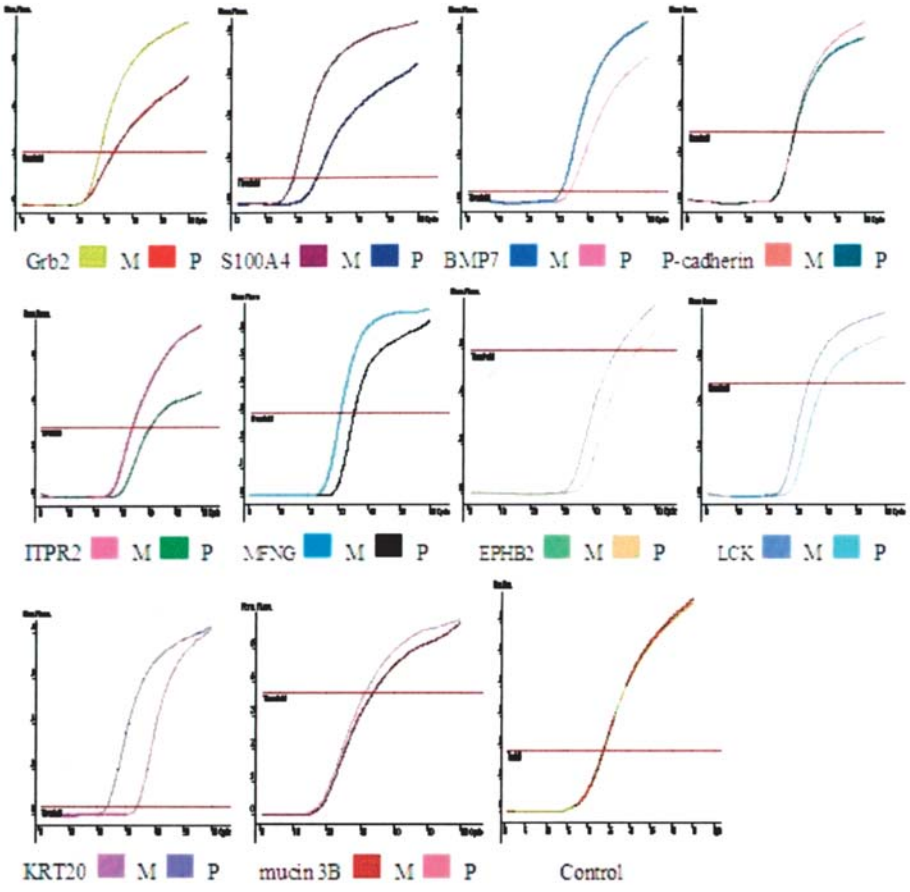

Figure 5. A coincidence between the real-time RT-PCR data and cDNA microarray data.

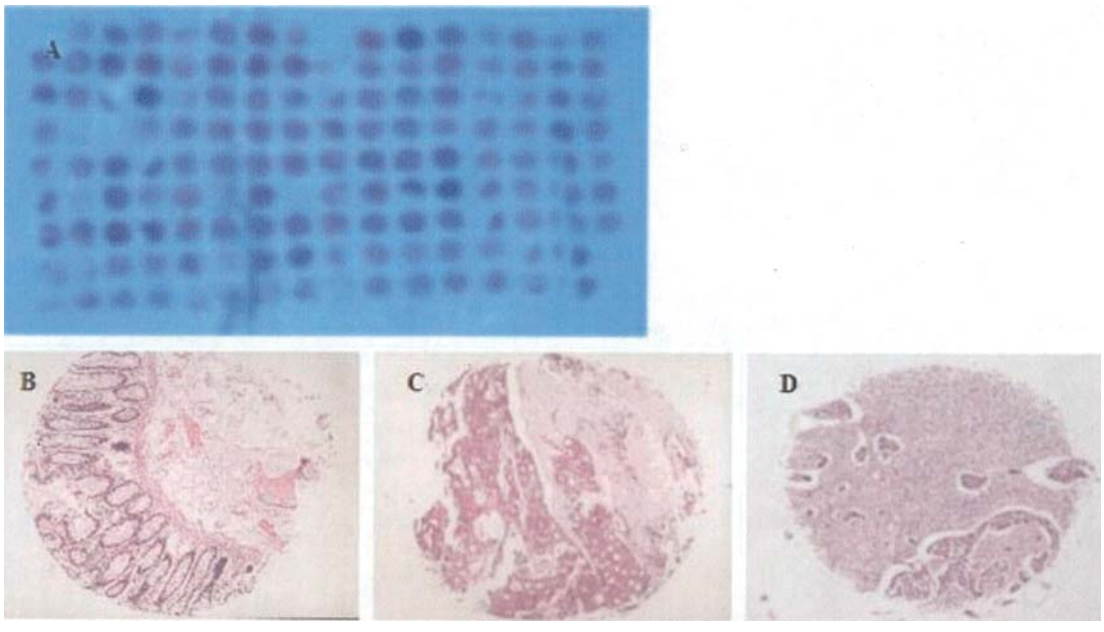

Figure 6. Tissue microarray (TMA) containing normal adjacent-cancer mucosa, primary tumor and metastases of 35 patients. A, the general view of TMA; B, normal tissues; C, primary tumor; D, lymph node metastases.

Since the data obtained from cDNA microarray, RT-PCR and TMA all revealed a higher expression of Grb2 in metastatic cells than in primary tumor cells, Grb2 must have a metastatic potential in the progress towards the metastasis of colorectal carcinoma. After using a Grb2-SH2 domain-binding antagonist on tumor cells, the motility of SW620 cells decreased (Fig. 9). This result confirmed the role of Grb2 in the pathway of metastasis and the importance of cDNA microarray and TMA.

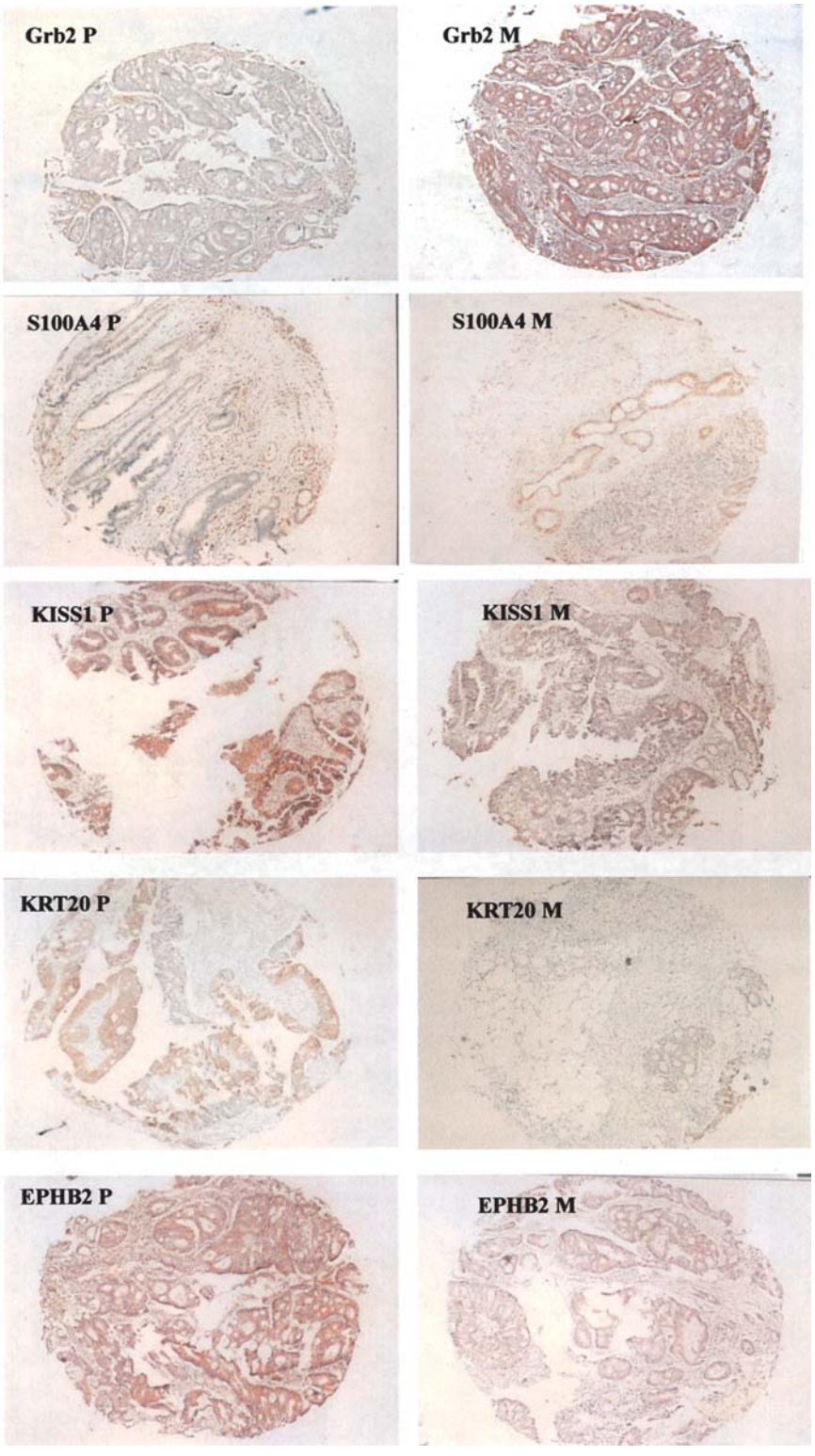

Figure 7. Representative examples of immunohistochemical staining for Grb2, S100A4, KISS1, EPHB2 and KRT20 (x20/200). N, normal tissue; P, primary tumor; M, nodal metastases. The percentage and intensity of the positive cells of KISS1, EPHB2 and KRT20 were lower while the percentage and intensity of the positive cells of Grb2 and S100A4 were higher in metastases than in primary tumor and normal tissues.

Discussion

To obtain precise information on the differences in gene expression profiles between cells of primary colorectal cancer and lymph node metastases, pure and sufficient populations of each type of cells is necessary because stroma cells play a certain role in carcinogenesis. Laser-capture microdissection is a good method to extract the desired cells from tissue specimens, although some non-malignant cells will be left. Implanting fresh tumor cells in nude mice is an effective way to get sufficient pure cells because cancer cells usually grow faster than non-malignant cells. By combining these two

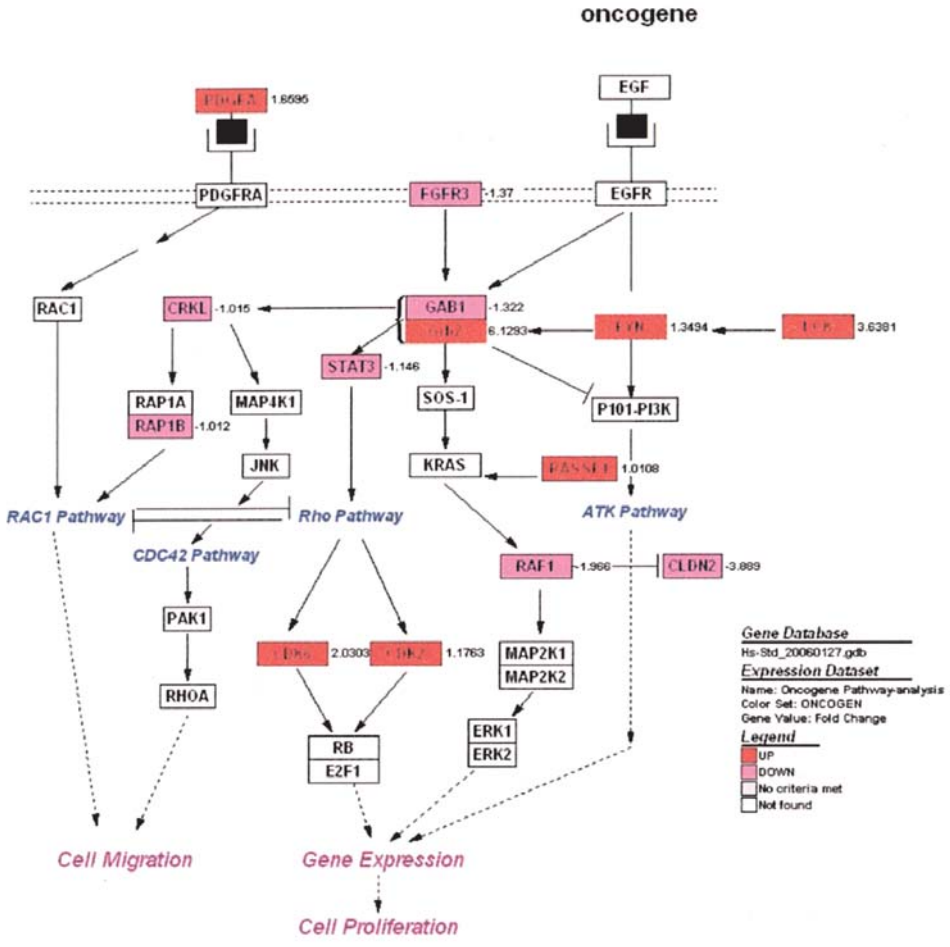

Figure 8. The pathways involved in the metastasis of colorectal carcinoma.

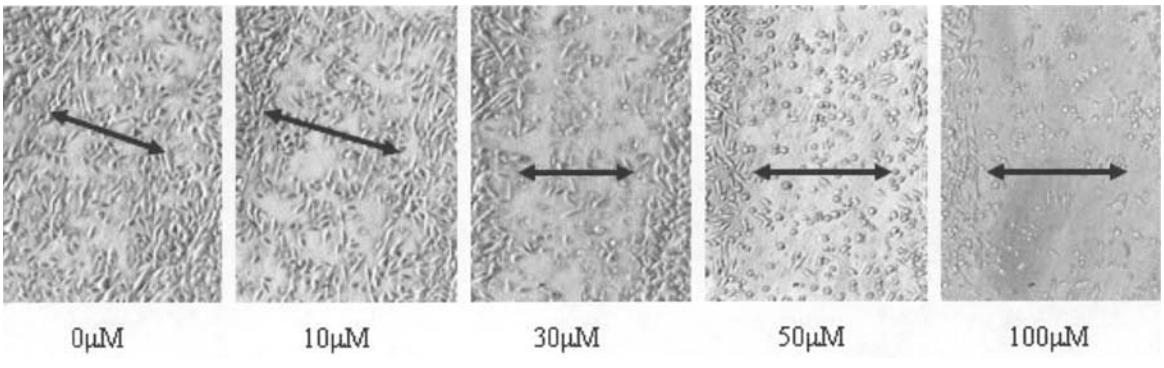

Figure 9. Inhibition of mobility of SW620 by a Grb2-SH2 antagonist, in whole cells as determined by the *in vitro* wound assay. The optimal concentration is 30 μM.

methods, microarray analysis can effectively identify metastasis-related genes since the interference of host cells is minimized. Furthermore, in order to investigate the levels of their proteins and to confirm its universality, large numbers of specimens are required. TMA is a powerful method which enables hundreds of cases to be detected at one time with the same standard. Thus, combining with TMA and sample preparation, microarray data become reliable and valuable.

Since metastasis arises from rare cells within the primary tumor and a cancer cell must complete at least 10 steps before a secondary tumor is colonized, metastatic cells must have a set of characteristics different from those of primary tumor cells. Studies have shown that metastatic cells have a higher capacity of proliferation, metastasis and invasion than primary tumor cells, which suggests that it is important to understand the underlying mechanism.

Using GO analysis and pathway-analysis, 376 genes were obtained from the 1327 genes. Among these genes, metastasis-associated gene (MTA; NM004689), metastasis suppressor 1 (MTSS1; NM014751) and KISS1 metastasis-suppressor

Table I. A representative list of up- and down-regulated genes in colorectal metastatic cancer cells.[a]

A, Up-regulated genes.

GO Category	Total genes	Overexpressed genes	Enrichment	LOG10 (p)	GO ID
Translation					
Lysyl-tRNA aminoacylation	1	1	50.296117	-1.70153	GO:0006430
Regulation of translational elongation	1	1	50.296117	-1.70153	GO:0006448
L-asparagine transport	1	1	50.296117	-1.70153	GO:0006867
Negative regulation of translational elongation	1	1	50.296117	-1.70153	GO:0045900
L-glutamine transport	1	1	50.296117	-1.70153	GO:0006868
Regulation of translation	66	4	3.048249	-1.37606	GO:0006445
Splicing					
mRNA splice site selection	5	2	20.118447	-2.42233	GO:0006376
Negative regulation of RNA metabolism	2	1	25.148058	-1.40482	GO:0051253
Negative regulation of mRNA processing	2	1	25.148058	-1.40482	GO:0050686
RNA stabilization	2	1	25.148058	-1.40482	GO:0043489
mRNA stabilization	2	1	25.148058	-1.40482	GO:0048255
mRNA catabolism nonsense-mediated decay	14	2	7.18516	-1.51436	GO:0000184
Negative regulation of nuclear mRNA splicing via spliceosome	1	1	50.296117	-1.70153	GO:0048025
Regulation of RNA metabolism	6	2	16.765372	-2.25195	GO:0051252
Spliceosome assembly	17	2	5.91719	-1.35672	GO:0000245
mRNA catabolism	17	2	5.91719	-1.35672	GO:0006402
mRNA export from nucleus	30	4	6.706149	-2.55701	GO:0006406
mRNA transport	31	4	6.489821	-2.50373	GO:0051028
RNA export from nucleus	38	4	5.294328	-2.18033	GO:0006405
RNA transport	39	4	5.158576	-2.14002	GO:0050658
Establishment of RNA localization	39	4	5.158576	-2.14002	GO:0051236
RNA localization	40	4	5.029612	-2.10094	GO:0006403
RNA splicing via transesterification reactions with bulged adenosine as nucleophile	110	6	2.743425	-1.65148	GO:0000377
Nuclear mRNA splicing via spliceosome	110	6	2.743425	-1.65148	GO:0000398
RNA splicing	140	7	2.514806	-1.66495	GO:0008380
mRNA processing	174	11	3.17964	-3.15562	GO:0006397
mRNA metabolism	196	13	3.335967	-3.84267	GO:0016071
RNA processing	297	15	2.540208	-3.06629	GO:0006396
RNA metabolism	370	19	2.582774	-3.84579	GO:0016070
Nucleotide metabolism					
Adenine transport	1	1	50.296117	-1.70153	GO:0015853
Purine transport	2	1	25.148058	-1.40482	GO:0006863
Glutathione biosynthesis	9	2	11.176915	-1.88882	GO:0006750
Nucleobase biosynthesis	9	2	11.176915	-1.88882	GO:0046112
Purine nucleoside monophosphate metabolism	11	2	9.144748	-1.7161	GO:0009126
Purine nucleoside monophosphate biosynthesis	11	2	9.144748	-1.7161	GO:0009127
Purine ribonucleoside monophosphate metabolism	11	2	9.144748	-1.7161	GO:0009167
Purine ribonucleoside monophosphate biosynthesis	11	2	9.144748	-1.7161	GO:0009168
Ribonucleoside monophosphate biosynthesis	17	2	5.91719	-1.35672	GO:0009156
Ribonucleoside monophosphate metabolism	17	2	5.91719	-1.35672	GO:0009161
Nucleoside monophosphate metabolism	18	2	5.588457	-1.31116	GO:0009123
Nucleoside monophosphate biosynthesis	18	2	5.588457	-1.31116	GO:0009124
Protein import into nucleus docking	16	3	9.430522	-2.44577	GO:0000059
Nucleobase nucleoside nucleotide and nucleic acid transport	49	5	5.132257	-2.55698	GO:0015931
NLS-bearing substrate import into nucleus	13	2	7.737864	-1.57567	GO:0006607
Nuclear import	54	4	3.725638	-1.65482	GO:0051170

Table 1A. Continued.

GO Category	Total genes	Overexpressed genes	Enrichment	LOG10 (p)	GO ID
Nuclear transport	96	8	4.191343	-3.19928	GO:0051169
Nucleocytoplasmic transport	103	8	3.906494	-2.99702	GO:0006913
Protein modification and degradation					
Peptide modification	1	1	50.296117	-1.70153	GO:0031179
DNA damage-induced protein phosphorylation	2	1	25.148058	-1.40482	GO:0006975
Basic amino acid transport	2	1	25.148058	-1.40482	GO:0015802
Protein amino acid farnesylation	2	1	25.148058	-1.40482	GO:0018347
Protein repair	2	1	25.148058	-1.40482	GO:0030091
Peptide metabolism	9	2	11.176915	-1.88882	GO:0006518
Amino acid transport	52	4	3.868932	-1.7091	GO:0006865
Protein import into nucleus	53	4	3.795933	-1.68163	GO:0006606
Amine transport	59	4	3.409906	-1.52972	GO:0015837
Protein import	65	4	3.095146	-1.39666	GO:0017038
Protein amino acid phosphorylation	506	17	1.68979	-1.62177	GO:0006468
Phosphorylation	589	18	1.537063	-1.34021	GO:0016310
Protein modification	1407	41	1.46563	-2.16065	GO:0006464
Biopolymer modification	1442	43	1.499815	-2.43319	GO:0043412
L-amino acid transport	14	2	7.18516	-1.51436	GO:0015807
Metabolism					
Glycine catabolism	5	2	20.118447	-2.42233	GO:0006546
Serine family amino acid catabolism	6	2	16.765372	-2.25195	GO:0009071
Glycine metabolism	11	2	9.144748	-1.7161	GO:0006544
Glutathione metabolism	12	2	8.382686	-1.64257	GO:0006749
Organic acid transport	67	5	3.753442	-1.97698	GO:0015849
Carboxylic acid transport	67	5	3.753442	-1.97698	GO:0046942
Steroid metabolism	137	7	2.569875	-1.71092	GO:0008202
Lipid metabolism	505	16	1.59354	-1.35504	GO:0006629
Phosphate metabolism	729	23	1.586846	-1.73459	GO:0006796
Cellular biosynthesis	858	25	1.465505	-1.47081	GO:0044249
Biosynthesis	969	27	1.40144	-1.34621	GO:0009058
Cellular protein metabolism	2576	65	1.269118	-1.77055	GO:0044267
Protein metabolism	2596	65	1.25934	-1.69977	GO:0019538
Cellular macromolecule metabolism	2615	65	1.25019	-1.63433	GO:0044260
Biopolymer metabolism	2289	69	1.516135	-4.01641	GO:0043283
Macromolecule metabolism	3503	91	1.306579	-2.93977	GO:0043170
Cellular metabolism	5945	134	1.133672	-1.84976	GO:0044237
Primary metabolism	5714	137	1.20591	-3.27693	GO:0044238
Glutamine family amino acid metabolism	37	3	4.078064	-1.43558	GO:0009064
Metabolism	6221	141	1.13997	-2.1385	GO:0008152
Cell-cycle progression					
Mitotic sister chromatid cohesion	1	1	50.296117	-1.70153	GO:0007064
G1 phase of mitotic cell cycle	17	2	5.91719	-1.35672	GO:0000080
G1 phase	17	2	5.91719	-1.35672	GO:0051318
Cell cycle arrest	60	5	4.191343	-2.17623	GO:0007050
Negative regulation of progression through cell cycle	147	9	3.079354	-2.57877	GO:0045786
Regulation of progression through cell cycle	418	17	2.045536	-2.39215	GO:0000074
Regulation of cell cycle	418	17	2.045536	-2.39215	GO:0051726
Cell cycle	618	20	1.627706	-1.66969	GO:0007049
Cellular physiological process	8259	184	1.120533	-3.80477	GO:0050875
Physiological process	9168	193	1.058808	-2.08053	GO:0007582

Table 1A. Continued.

GO Category	Total genes	Overexpressed genes	Enrichment	LOG10 (p)	GO ID
Signaling pathway					
T cell receptor signaling pathway	1	1	50.296117	-1.70153	GO:0050852
Regulation of T cell receptor signaling pathway	1	1	50.296117	-1.70153	GO:0050856
Regulation of T cell receptor signaling pathway	1	1	50.296117	-1.70153	GO:0050862
Antigen receptor mediated signaling pathway	2	1	25.148058	-1.40482	GO:0050854
Regulation of antigen receptor mediated signaling pathway	2	1	25.148058	-1.40482	GO:0050857
Regulation of JNK activity	16	2	6.287015	-1.40547	GO:0043506
Ras protein signal transduction	32	3	4.715261	-1.59935	GO:0007265
Others					
Zinc ion homeostasis	1	1	50.296117	-1.70153	GO:0006882
Canalicular bile acid transport	1	1	50.296117	-1.70153	GO:0015722
Cytoplasmic transport	1	1	50.296117	-1.70153	GO:0016482
Response to cold	2	1	25.148058	-1.40482	GO:0009409
Neuron lineage restriction	2	1	25.148058	-1.40482	GO:0042055
Neuron fate commitment	2	1	25.148058	-1.40482	GO:0048663
Sequestering of calcium ion	2	1	25.148058	-1.40482	GO:0051208
Chromosome organization and biogenesis	225	9	2.011845	-1.44688	GO:0051276

B, Down-regulated genes.

GO Category	Total genes	Underexpressed genes	Enrichment	LOG10 (p)	GO ID
Membrane signaling and cell adhesion					
Inactivation of MAPK activity during osmolarity sensing	1	1	28.780556	-1.459099	GO:0000173
CDP-choline pathway	1	1	28.780556	-1.459099	GO:0006657
Osmosensory signaling pathway via substrate-bound cell migration	1	1	28.780556	-1.459099	GO:0007234
Cell extension	4	2	14.390278	-2.16143	GO:0006930
Substrate-bound cell migration	6	2	9.593519	-1.783588	GO:0006929
Cell-mediated immune response	22	3	3.924621	-1.405927	GO:0042087
Cell-matrix adhesion	60	6	2.878056	-1.758569	GO:0007160
Cell-substrate adhesion	60	6	2.878056	-1.758569	GO:0031589
Negative regulation of cell proliferation	137	12	2.520925	-2.538451	GO:0008285
Transmembrane receptor protein tyrosine kinase signaling pathway	118	10	2.43903	-2.101311	GO:0007169
Skeletal development	122	10	2.359062	-2.003461	GO:0001501
Small GTPase-mediated signal transduction	230	18	2.252391	-2.959368	GO:0007264
Enzyme linked receptor protein signaling pathway	167	13	2.240403	-2.263691	GO:0007167
Cell motility	194	14	2.076947	-2.111639	GO:0006928
Locomotion	194	14	2.076947	-2.111639	GO:0040011
Localization of cell	194	14	2.076947	-2.111639	GO:0051674
Regulation of cell proliferation	264	15	1.635259	-1.374646	GO:0042127
Cell adhesion	562	31	1.58754	-2.144182	GO:0007155
Chromatin modifications					
Chromatin silencing at rDNA	1	1	28.780556	-1.459099	GO:0000183
Chromatin silencing at telomere	1	1	28.780556	-1.459099	GO:0006348
Telomeric heterochromatin formation	1	1	28.780556	-1.459099	GO:0031509
RNA splicing					
Primary microRNA processing	1	1	28.780556	-1.459099	GO:0031053
miRNA-mediated gene silencing	1	1	28.780556	-1.459099	GO:0035195
miRNA-mediated gene silencing production of miRNAs	1	1	28.780556	-1.459099	GO:0035196

Table 1B. Continued.

GO Category	Total genes	Underexpressed genes	Enrichment	LOG10 (p)	GO ID
Response to dsRNA	1	1	28.780556	-1.459099	GO:0043331
mRNA catabolism	17	3	5.078922	-1.705706	GO:0006402
RNA catabolism	33	4	3.488552	-1.57683	GO:0006401
Immune response					
Induction of host defense response	1	1	28.780556	-1.459099	GO:0044416
Negative regulation of MHC class II biosynthesis	1	1	28.780556	-1.459099	GO:0045347
Interferon-α biosynthesis	1	1	28.780556	-1.459099	GO:0045349
Induction of host immune response by virus	1	1	28.780556	-1.459099	GO:0046730
Plasma membrane to endosome transport	1	1	28.780556	-1.459099	GO:0048227
T-helper 2 type immune response	5	2	11.512222	-1.949645	GO:0042092
Antigen processing endogenous antigen via MHC class I	10	2	5.756111	-1.346303	GO:0019885
Acute-phase response	26	5	5.534722	-2.751298	GO:0006953
Antigen processing	23	4	5.005314	-2.123905	GO:0030333
Antigen presentation	34	4	3.385948	-1.534153	GO:0019882
Metabolism and biosynthesis					
Negative regulation of nitric oxide biosynthesis	1	1	28.780556	-1.459099	GO:0045019
Glycogen catabolism	4	2	14.390278	-2.16143	GO:0005980
Glucan catabolism	5	2	11.512222	-1.949645	GO:0009251
Regulation of lipid metabolism	9	3	9.593519	-2.524469	GO:0019216
Arginine catabolism	6	2	9.593519	-1.783588	GO:0006527
Triacylglycerol metabolism	8	2	7.195139	-1.5325	GO:0006641
Interferon-γ biosynthesis	9	2	6.395679	-1.433299	GO:0042095
Glutamine family amino acid catabolism	14	3	6.167262	-1.943718	GO:0009065
Neutral lipid metabolism	10	2	5.756111	-1.346303	GO:0006638
Acylglycerol metabolism	10	2	5.756111	-1.346303	GO:0006639
Glutamine family amino acid biosynthesis	10	2	5.756111	-1.346303	GO:0009084
Energy reserve metabolism	33	4	3.488552	-1.57683	GO:0006112
Glutamine family amino acid metabolism	37	4	3.111411	-1.415548	GO:0009064
Steroid biosynthesis	65	6	2.656667	-1.603281	GO:0006694
Glycoprotein biosynthesis	115	8	2.002126	-1.329949	GO:0009101
Fatty acid metabolism	131	9	1.97729	-1.411505	GO:0006631
Lipid biosynthesis	177	12	1.951224	-1.686988	GO:0008610
Cellular lipid metabolism	399	26	1.875425	-2.817255	GO:0044255
Lipid metabolism	505	30	1.709736	-2.546995	GO:0006629
Sterol biosynthesis	25	4	4.604889	-1.992662	GO:0016126
Cholesterol biosynthesis	21	3	4.111508	-1.458593	GO:0006695
Ion					
Copper ion homeostasis	4	3	21.585417	-3.790113	GO:0006878
Response to metal ion	8	2	7.195139	-1.5325	GO:0010038
Copper ion transport	10	2	5.756111	-1.346303	GO:0006825
Iron ion homeostasis	18	3	4.796759	-1.637614	GO:0006879
Transition metal ion homeostasis	22	5	6.541035	-3.099288	GO:0046916
Response to inorganic substance	9	2	6.395679	-1.433299	GO:0010035
Response					
Response to lipid hydroperoxide	1	1	28.780556	-1.459099	GO:0006982
Response to unfolded protein	48	5	2.997975	-1.605237	GO:0006986
Organ development	529	30	1.632168	-2.256436	GO:0048513
Response to pest pathogen or parasite	496	26	1.508658	-1.624834	GO:0009613
Response to wounding	363	19	1.50642	-1.307728	GO:0009611
Response to other organism	523	27	1.485803	-1.594345	GO:0051707
Response to stress	946	45	1.369054	-1.739123	GO:0006950

Table 1B. Continued.

GO Category	Total genes	Underexpressed genes	Enrichment	LOG10 (p)	GO ID
Response to stimulus	1822	76	1.200506	-1.344846	GO:0050896
Others					
Ribosomal protein import into nucleus	1	1	28.780556	-1.459099	GO:0006610
Fat body development	1	1	28.780556	-1.459099	GO:0007503
Stem cell maintenance	1	1	28.780556	-1.459099	GO:0019827
Neuromuscular physiological process	1	1	28.780556	-1.459099	GO:0050905
Negative regulation of NF-κB import into nucleus	4	2	14.390278	-2.16143	GO:0042347
Negative regulation of protein import into nucleus	8	2	7.195139	-1.5325	GO:0042308
Cytoplasmic sequestering of protein	8	2	7.195139	-1.5325	GO:0051220
Negative regulation of protein transport	9	2	6.395679	-1.433299	GO:0051224
Maintenance of localization	15	3	5.756111	-1.857961	GO:0051235

[a]The 190 genes listed show a 4-fold up-regulated expression in metastatic cancer cells compared with that in primary cancer cells. The 186 genes show a 4-fold down-regulated expression in metastatic cancer cells compared with that in primary cancer cells.

Table II. Protein levels in metastases and primary tumors.

A, Staining results of metastases compared with the primary tumors after dichotomizing the results for the 35 patients of the study population with nodal metastases.

		Concordance		Discordance	
Primary	N	-	+	-	+
Nodal metastasis		-	+	+	-
S100A4	35	6	20	9	0
GrB2	35	3	22	7	3
KISS1	35	3	20	0	12
CK20	35	5	17	1	12
EphB2	35	10	12	3	10

B, Different levels of positive staining of the five proteins in the concordant patients.

			Different levels	
Primary	N	Same level	High	Low
Nodal metastasis			Low	High
S100A4	20	14	1	5
GrB2	22	7	0	15
KISS1	20	8	12	0
CK20	17	10	7	0
EphB2	12	4	7	1

Table III. Relationship between positive staining of Grb2 in the primary tumor and the metastases and pathological characteristics.

	N	Grb2	
		+	>
Sex			
Male	24	14	14
Female	11	8	8
Age			
>60	14	11	11
40-60	11	8	9
≤40	10	3	2
Type			
Adenocarcinoma	30	20	19
Mucous	4	2	3
Ring	1	0	1
Others	0	0	0
Differentiation of adenocarcinoma			
High	1	0	1
Modern	19	15	11
Low	10	5	10
Distant metastasis			
Positive	21	14	17[a]
Negative	14	8	5

+, Positive staining of Grb2 in the primary tumor; >, elevated levels of Grb2 staining in the metastasis site compared with in the primary site. [a]P<0.05.

(KISS1; NM002256) were first discovered as metastasis-related genes. The overexpression of MTA1 mRNA is directly correlated with metastatic potential in gastrointestinal carcinoma (7). KISS1 is expressed in normal colonic mucosa, though its reduced expression is responsible for tumor invasion, distant metastasis and a worse prognosis in gastric carcinoma (8). MTSS1 is located in a genomic region with a frequent loss of heterozygosity (8q22) and is expressed abundantly in the normal gastric mucosa, suggesting its role in gastric carcinogenesis (9). In addition, S100A4

(NM002961), which was up-regulated in the present study, is known to modify the cytoskeleton and focal adhesion and to trigger several other events in tumor cells (10). A higher expression of the S100A4 protein is closely associated with tumor progress and distant metastasis in many types of cancers (11).

A number of genes showing a down-regulated expression in colorectal metastatic cells have been associated with metastasis directly or indirectly, which include a decay accelerating factor for complement (DAF; NM000574), a cell-membrane-complement regulator and two adhesion molecules, i.e. claudin2 (CLDN2; NM020384) and several metabolism-related genes including carbonic anhydrase XII (CA12; NM00128), UDP-N-acetyl-α-D-galactosamine: polypeptide N-acetylgalactosaminyltransferase 3 (GalNAc-T3; NM004482), catechol-O-methyltransferase (COMT; NM000754) and signal transduction genes: annexin A10 (ANXA10; NM007193), annexin A1 (ANXA1; 000700) and Keratin 20 (KRT20; NM019010). DAF is significantly elevated in patients with colorectal cancer and can be excreted into the stool and thus can be detected by ELISA (12). Our present study showed that adenocarcinoma exposed to complementary attack in the early stages may up-regulate DAF in order to protect malignant cells from complementary lysis. This is similar to the results obtained by Nowicki *et al* (13). CLDN2 is critical for maintaining cell-cell adhesions in epithelial cell sheets and acts as selective barriers, because it is down-regulated markedly by Raf-1, which activates signal transduction and stimulates cell proliferation. CLDN2 is increased in the early phase of carcinogenesis, though is reduced during progression to invasive diseases (14). Most of the gene encoded enzymes necessary for cell growth and metabolism are involved in metastasis, which is consistent with the observation that CA12, a hypoxia-inducible gene, is a marker of good prognosis in invasive breast carcinoma, which has an inverse relationship with VEGF (vascular endothelial growth factor) (15). A low expression of GALNT3 is associated with a poorly differentiated tumor, poor pathological stage and nodal metastases in lung carcinoma patients (16). A low activity of COMT may contribute to the progression of breast cancer because it is responsible for detoxification of catecholestrogens which may prevent the genesis and arrest the progress of the disease (17). Therefore, the abnormity of enzyme metabolism may be a crucial step for metastasis in various cancers. Signal molecules: ANXA10, a calcium-binding protein participating in diverse biological processes, is a marker of cell differentiation and growth arrest since the down-regulation of ANXA10 is related to vascular invasion and progression of hepatic carcinoma and poor prognosis and perhaps repressed by S100A4 and mtp53 (18). The down-regulation of ANXA1 is significantly associated with advanced T stage, lymph node metastases, advanced disease stage and poor differentiation in HNSCC, which identifies ANXA1 as an effective differentiation marker (19). EPHB2, a receptor tyrosine kinase, may achieve its tumor-suppressing function through the regulation of cell survival, adhesion and migration since a progressive loss of EPHB2 is accompanied by the progress towards the metastases of colorectal carcinoma (20). Notably, the KRT20 gene was down-regulated in metastatic cells rather than in primary cancer cells in microarray, RT-PCR and IHC data. IHC also showed that KRT20 was reduced in cancer tissues, which was consistent with the results from previous publications (21). Hence KRT20 may be a useful prognostic marker, which gradually decreases with the progress to metastasis of colorectal carcinoma.

Among other genes showing up-regulated expression in metastatic cells, we noted the presence of the growth factor receptor-bound protein gene (Grb2; NM002086), lymphocyte-specific protein tyrosine kinase gene (LCK; NM005356), EPHB4 gene (EPHB4; NM004444), LAT1-3TM gene (LAT1-3TM; NM031211), cyclin L1 gene (CCNL1; BX538238), cathepsin D (CTSD; NM001909), bone morphogenetic protein 7 (BMP7; NM001719) and cyclin-dependent kinase 6 gene (CDK6; NM001259). Grb2 is an SH2 domain-containing docking module that participates in the signaling of numerous oncogenic growth factor receptor protein-tyrosine kinases (PTKs), the de-regulation of which contributes to cellular transformation and metastasis (22). LCK sequence appears highly homologous to oncogene p60-src which is often implicated in human cancers and could favor metastases by facilitating the loss of adhesion (23). EPHB4 is a candidate gene of metastatic potential because in EPHB4 knockout mice it leads to nearly 80% reduction in tumor and reduced tumor microvasculature (24). LAT1-3TM has a similar sequence to the amino acid transporter LAT1, the high expression of which is related to invasion and liver metastasis tumors (25). The amplification of cyclin L1, a candidate oncogene, is associated with lymph node metastases in head and neck squamous cell carcinoma according to FISH (fluorescence *in situ* hybridization) and TMA (26). CDK6 is required for cell cycle progression (G1-S phase transition) by binding D cyclin and forming D cyclin/CDK6 complex. CTSD expression is a possible predictor of lymph node metastases in submucosal colorectal cancer (27). Since BMP7 was able to inhibit serum starvation-induced apoptosis and induce motility and invasiveness of PC3 prostate cells, BMP7 could contribute to cancer cell growth and metastasis in the case of prostate cancer (28). The enhanced expression of these genes may play a direct or indirect role in the mechanisms of colorectal cancer metastasis including accelerated metabolism, impaired regulation of cell cycle, imbalance of adhesion and disadhesion and the deregulation of phosphorylation and transporters.

In this study, we selected five proteins (GrB2, S100A4, KRT20, KISS1 and EPHB2), as discussed above, to detect their expression levels using TMA and IHC. The levels of GrB2 and S100A4 were higher in metastases than in primary tumors and the levels of KRT20, KISS1 and EPHB2 were apparently decreased, or even undetectable, in metastases compared with primary tumors in most of the cases, in agreement with the results from previous reports (15,34-36).

In our experiment, we noted that Grb2 had the highest ratio and enrichment. The IHC results also confirmed the reliability in a large number of tumor tissues and revealed that a tumor in patients with a higher expression in nodal metastases than in the primary tumor easily metastasizes to the liver. Thus, we used Grb2 as the target to investigate pathways based on the original data. Grb2 especially mediates the MAPKK, Akt and RHo pathways. Most of the

genes involved in these pathways were elevated in metastatic cells compared with primary tumor cells, which suggests a critical role of Grb2-mediated pathways in the process of metastasis.

Therapeutic intervention has been approached through the down-regulation of the affected pathways including the Grb-SH2 signal pathway (29). After using a Grb2-SH2 domain-binding antagonist, SW620 cells with a high metastatic potential showed a slower motility at the concentration of 30 mM. Thus, it is possible that Grb2 contributes to high-grade metastasis.

In conclusion, our results reveal not only new information about metastasis-related genes but also a novel association between known genes and metastasis. The identified relationship between cancer characteristics and genes will help to further investigate the function of the genes. In addition, our observations that the Grb2-mediated MAPK pathway plays a key role in the progress and function of metastasis of colorectal carcinoma may prove useful for identifying novel therapeutic targets.

References

1. Debies MT and Welch DR: Genetic basis of human breast cancer metastasis. J Mamm Gland Biol Neopl 6: 441-451, 2002.
2. Martin MD, Fischbach K, Osborne CK, Mohsin SK, Allred DC and O'Connell P: Loss of heterozygosity events impeding breast cancer metastasis contain the MTA1 gene. Cancer Res 61: 3578-3580, 2001.
3. Ornstein DK, Gillespie JW, Paweletz CP, Duray PH, Herring J, Vocke CD, Topalian SL, Bostwick DG, Linehan WM, Petricoin EF III and Emmert-Buck MR: Proteomic analysis of laser capture microdissected human prostate cancer and *in vitro* prostate cell lines. Electrophoresis 21: 2235-2242, 2000.
4. Sugiyama Y, Farrow B, Murillo C, Li J, Watanabe H, Sugiyama K and Evers BM: Analysis of differential gene expression patterns in colon cancer and cancer stroma using microdissected tissues. Gastroenterology 128: 480-486, 2005.
5. Yu GZ, Zhu MH, Zhu Z, Ni CR, Zheng JM and Li FM: Expression of ATM protein and its relationship with p53 in pancreatic carcinoma with tissue array. Pancreas 28: 421-426, 2004.
6. Song YL, Roller PP and Long YQ: Development of l-3-aminotyrosine suitably protected for the synthesis of a novel nonphosphorylated hexapeptide with low-nanomolar Grb2-SH2 domain-binding affinity. Bioorg Med Chem Lett 14: 3205-3208, 2004.
7. Toh Y, Pencil SD and Nicolson GL: A novel candidate metastasis-associated gene, mta1, differentially expressed in highly metastatic mammary adenocarcinoma cell lines. cDNA cloning, expression, and protein analyses. J Biol Chem 269: 22958-22963, 1994.
8. Dhar DK, Naora H, Kubota H, Maruyama R, Yoshimura H, Tonomoto Y, Tachibana M, Ono T, Otani H and Nagasue N: Downregulation of KiSS-1 expression is responsible for tumor invasion and worse prognosis in gastric carcinoma. Int J Cancer 111: 868-872, 2004.
9. Yamashita S, Tsujino Y, Moriguchi K, Tatematsu M and Ushijima T: Chemical genomic screening for methylation-silenced genes in gastric cancer cell lines using 5-aza-2'-deoxycytidine treatment and oligonucleotide microarray. Cancer Sci 97: 64-71, 2006.
10. Belot N, Pochet R, Heizmann CW, Kiss R and Decaestecker C: Extracellular S100A4 stimulates the migration rate of astrocytic tumor cells by modifying the organization of their actin cytoskeleton. Biochim Biophys Acta 1600: 74-83, 2002.
11. Flatmark K, Pedersen KB, Nesland JM, Rasmussen H, Aamodt G, Mikalsen SO, Bjornland K, Fodstad O and Maelandsmo GM: Nuclear localization of the metastasis-related protein S100A4 correlates with tumour stage in colorectal cancer. J Pathol 200: 589-595, 2003.
12. Okazaki H, Mizuno M, Nasu J, Makidono C, Hiraoka S, Yamamoto K, Okada H, Fujita T, Tsuji T and Shiratori Y: Difference in Ulex europaeus agglutinin I-binding activity of decay-accelerating factor detected in the stools of patients with colorectal cancer and ulcerative colitis. J Lab Clin Med 143: 169-174, 2004.
13. Nowicki S, Nowicki B, Pham T, Hasan R and Nagamani M: Expression of decay accelerating factor in endometrial adenocarcinoma is inversely related to the stage of tumor. Am J Reprod Immunol 46: 144-148, 2001.
14. Sobel G, Paska C, Szabo I, Kiss A, Kadar A and Schaff Z: Increased expression of claudins in cervical squamous intraepithelial neoplasia and invasive carcinoma. Hum Pathol 36: 162-169, 2005.
15. Kivela AJ, Parkkila S, Saarnio J, Karttunen TJ, Kivela J, Parkkila AK, Bartosova M, Mucha V, Novak M, Waheed A, Sly WS, Rajaniemi H, Pastorekova S and Pastorek J: Expression of von Hippel-Lindau tumor suppressor and tumor-associated carbonic anhydrases IX and XII in normal and neoplastic colorectal mucosa. World J Gastroenterol 11: 2616-2625, 2005.
16. Gu C, Oyama T, Osaki T, Li J, Takenoyama M, Izumi H, Sugio K, Kohno K and Yasumoto K: Low expression of polypeptide GalNAc N-acetylgalactosaminyl transferase-3 in lung adenocarcinoma: impact on poor prognosis and early recurrence. Br J Cancer 90: 436-442, 2004.
17. Matsui A, Ikeda T, Enomoto K, Nakashima H, Omae K, Watanabe M, Hibi T and Kitajima M: Progression of human breast cancers to the metastatic state is linked to genotypes of catechol-O-methyltransferase. Cancer Lett 150: 23-31, 2000.
18. Liu SH, Lin CY, Peng SY, Jeng YM, Pan HW, Lai PL, Liu CL and Hsu HC: Down-regulation of annexin A10 in hepatocellular carcinoma is associated with vascular invasion, early recurrence, and poor prognosis in synergy with p53 mutation. Am J Pathol 160: 1831-1837, 2002.
19. Garcia Pedrero JM, Fernandez MP, Morgan RO, Herrero Zapatero A, Gonzalez MV, Suarez Nieto C and Rodrigo JP: Annexin A1 down-regulation in head and neck cancer is associated with epithelial differentiation status. Am J Pathol 164: 73-79, 2004.
20. Guo DL, Zhang J, Yuen ST, Tsui WY, Chan AS, Ho C, Ji J, Leung SY and Chen X: Reduced expression of EphB2 that parallels invasion and metastasis in colorectal tumors. Carcinogenesis 27: 454-464, 2006.
21. Frederiksen CM, Knudsen S, Laurberg S and Ontoft TF: Classification of Dukes' B and C colorectal cancers using expression arrays. J Cancer Res Clin Oncol 129: 263-271, 2003.
22. Saucier C, Papavasiliou V, Palazzo A, Naujokas MA, Kremer R and Park M: Use of signal specific receptor tyrosine kinase oncoproteins reveals that pathways downstream from Grb2 or Shc are sufficient for cell transformation and metastasis. Oncogene 21: 1800-1811, 2002.
23. Rouer E: Expression of the p56lck by colon tumors: a marker of their invasive capacity? Bull Cancer 91: 928-940, 2004.
24. Xia G, Kumar SR, Stein JP, Singh J, Krasnoperov V, Zhu S, Hassanieh L, Smith DL, Buscarini M, Broek D, Quinn DI, Weaver FA and Gill PS: EphB4 receptor tyrosine kinase is expressed in bladder cancer and provides signals for cell survival. Oncogene 25: 769-780, 2006.
25. Tamai S, Masuda H, Ishii Y, Suzuki S, Kanai Y and Endou H: Expression of L-type amino acid transporter 1 in a rat model of liver metastasis: positive correlation with tumor size. Cancer Detect Prev 25: 439-445, 2001.
26. Sticht C, Hofele C, Flechtenmacher C, Bosch FX, Freier K, Lichter P and Joos S: Amplification of Cyclin L1 is associated with lymph node metastases in head and neck squamous cell carcinoma (HNSCC). Br J Cancer 92: 770-774, 2005.
27. Oh-e H, Tanaka S, Kitadai Y, Shimamoto F, Yoshihara M and Haruma K: Cathepsin D expression as a possible predictor of lymph node metastasis in submucosal colorectal cancer. Eur J Cancer 37: 180-188, 2001.
28. Yang S, Zhong C, Frenkel B, Reddi AH and Roy-Burman P: Diverse biological effect and Smad signaling of bone morphogenetic protein 7 in prostate tumor cells. Cancer Res 65: 5769-5777, 2005.
29. Dharmawardana PG, Peruzzi B, Giubellino A, Burke TR Jr and Bottaro DP: Molecular targeting of growth factor receptor-bound 2 (Grb2) as an anti-cancer strategy. Anticancer Drugs 17: 13-20, 2006.